



# In situ observation of microstructural development during electron irradiation in $\text{Al}_2\text{O}_3$ containing $\text{Cr}_2\text{O}_3$ or $\text{TiO}_2$

K. Nakata <sup>a,\*</sup>, Y. Katano <sup>b</sup>, K. Noda <sup>b</sup>

<sup>a</sup> *Second Department of Materials, Hitachi Research Laboratory, Hitachi Ltd., Hitachi-shi, Ibaraki 317, Japan*

<sup>b</sup> *Department of Materials Science and Engineering, Japan Atomic Energy Research Institute, Tokai-mura, Ibaraki 319-11, Japan*

## Abstract

In order to clarify the effects of  $\text{Cr}^{3+}$  and  $\text{Ti}^{4+}$  additions on damage structural development, pure and 1 mol% $\text{Cr}_2\text{O}_3$  - or 1 mol% $\text{TiO}_2$ -doped  $\text{Al}_2\text{O}_3$  have been irradiated with 400 keV electrons at temperatures from 293 to 1273 K. Dislocation loops and plate-shaped cavities are formed on (0 0 0 1) planes in the pure  $\text{Al}_2\text{O}_3$  sample. The damaged area, in which the loops are formed, expands outward from the central part of the electron beam during irradiation above 973 K. Although the expansion of the damaged area is also observed in the  $\text{Cr}_2\text{O}_3$ -doped sample, the expansion occurs at higher temperatures of 1073 K and the expansion rate is much smaller than that observed in pure sample. Cavities are formed in the  $\text{Cr}_2\text{O}_3$ -doped sample at a high density compared with the pure sample, but they hardly grow with irradiation dose, resulting in retention of very small size at higher doses than  $7.2 \times 10^{26}$  e/m<sup>2</sup>. The dislocation loop and cavity formation in the  $\text{TiO}_2$ -doped sample are similar to those in the pure sample. © 1998 Elsevier Science B.V. All rights reserved.

## 1. Introduction

Alumina,  $\text{Al}_2\text{O}_3$ , is one of the candidate materials for insulators and RF windows of fusion reactors [1], because of its excellent electrical resistivity and thermal conductivity. Studies of  $\text{Al}_2\text{O}_3$  for fusion reactor materials have focused on radiation effects on physical properties, mechanical properties and dimensional stability [2,3]. The volume swelling induced by displacement damage has been studied over a wide temperature range by electron, ion and neutron irradiations [4–8].

It is well known that electrical and thermal conductivities strongly depend on the species of dopants, like  $\text{Ti}^{4+}$ ,  $\text{Si}^{4+}$ ,  $\text{Cr}^{3+}$ ,  $\text{Ni}^{2+}$  or  $\text{Fe}^{2+}$ , in  $\text{Al}_2\text{O}_3$  [9]. Indeed, small amount of doped  $\text{Cr}_2\text{O}_3$  reduces radiation-induced conductivity (RIC) in  $\text{Al}_2\text{O}_3$  [10,11]. However, the effects of these dopants on mechanical properties and dimensional stability are not clear.

The objective in this study is to make a fundamental investigation of the effects of  $\text{Cr}_2\text{O}_3$  or  $\text{TiO}_2$  additions on

radiation-induced microstructural development in  $\text{Al}_2\text{O}_3$  using electron irradiation in a transmission electron microscope (TEM). These two dopants have been indicated to have beneficial effects on electrical conductivity in  $\text{Al}_2\text{O}_3$  [10,11].

## 2. Experimental procedure

Materials used were single crystal  $\alpha$ - $\text{Al}_2\text{O}_3$  (nominal purity; 99.9%) and  $\alpha$ - $\text{Al}_2\text{O}_3$  containing 1 mol%  $\text{Cr}_2\text{O}_3$  or  $\text{TiO}_2$ , which were supplied by Rare Metallic; the main impurities were C, Fe and Ca [12]. After annealing in vacuum at 1423 K for 3.6 ks, disks, 3 mm in diameter and 0.2 mm thick, were cut with faces of (0 0 0 1) for the pure and  $\text{Cr}_2\text{O}_3$ -doped samples, and (2  $\bar{1}$   $\bar{1}$  0) for the  $\text{TiO}_2$ -doped sample. Thin foils for electron irradiation and TEM observation were prepared by an Ar-ion sputtering method at room temperature. Anneal-out treatment of the induced defects was not carried out after the sputtering. No precipitates concerning with Cr or Ti could be found by TEM observation.

Electron irradiation and damage structure observation were made at temperatures from 293 to 1373 K with

\* Corresponding author. Tel.: +81 294 23 5771; fax: +81 294 23 6952; e-mail: nakataki@hrl.hitachi.co.jp.

400 keV electrons by a TEM. The irradiation beam was focused to about 600 nm diameter with an electron flux of  $1.0 \times 10^{24}$  e/m<sup>2</sup>s. Since the beam intensity had Gaussian distribution, the width of half maximum was approximately 200 nm. The irradiation was continued up to about  $1.2 \times 10^{27}$  e/m<sup>2</sup>. Irradiation temperature was controlled with an accuracy of  $\pm 2$  K using a hot stage during the irradiation. Foil thickness in the irradiated area was about 900 nm as determined by a thickness fringe technique [13]. Since the damaged area, in which radiation-induced defect clusters were formed by electron irradiation, was slightly elliptical in shape, the diameter of the damaged area was represented by its major axis.

### 3. Results and discussion

Dislocation loops are formed by irradiation at temperatures from 293 to 1373 K and cavities are found above 873 K in the pure, Cr<sub>2</sub>O<sub>3</sub>-doped and TiO<sub>2</sub>-doped samples. Figs. 1 and 2 show the microstructural development during irradiation at 973 K in the pure and Cr<sub>2</sub>O<sub>3</sub>-doped samples, respectively. The direction of the incident electron beam is  $[4\ 0\ \bar{4}\ 1]$  and  $[3\ \bar{1}\ 2\ \bar{1}]$  for the pure and Cr<sub>2</sub>O<sub>3</sub>-doped samples, respectively. The dislocation loops in the pure sample accompany a large strain field, judged from dark contrast of TEM micrographs. The loops are lying on (0 0 0 1) planes, and are seemed to be an interstitial type according to the inside-outside contrast analysis. A high density of black dots are observed in the matrix and inside the dislocation

loops after the  $7.2 \times 10^{26}$  e/m<sup>2</sup> irradiation. The black dots were confirmed to be in the foils by stereomicroscopy, and also confirmed to be cavities by an under- and over-focus contrast method. Precipitates on the surfaces can be seen after the  $7.2 \times 10^{26}$  e/m<sup>2</sup> irradiation. The precipitation takes place in a narrow temperature range around 973 K, and no precipitates are observed in the irradiation at 1073 K and above. Similar surface precipitates had been reported in Al<sub>2</sub>O<sub>3</sub> irradiated in an HVEM and these were concluded to be metallic Al [8,14]. The damage structure development in the TiO<sub>2</sub>-doped sample is similar to that in the pure sample (data are not shown). Dislocation loops are also formed on (0 0 0 1) planes in the Cr<sub>2</sub>O<sub>3</sub>-doped sample, but the growth rate is fairly small. A large strain appears around the damaged area in which the loops are formed. The foil are thinned during irradiation, and pitted after  $7.2 \times 10^{26}$  e/m<sup>2</sup>. No precipitates on the surfaces are found in the Cr<sub>2</sub>O<sub>3</sub>-doped sample at any irradiation temperatures tested.

Electron dose dependence of the diameter of the damaged area is shown in Fig. 3 for the pure and Cr<sub>2</sub>O<sub>3</sub>-doped samples at various irradiation temperatures. While little expansion of damaged area is found at 293 K, the expansion rate increases with irradiation temperature above 973 K in the pure sample. The diameter of the damaged area is proportional to the square root of the irradiation time (or fluence): its proportional constants are 22.5, 30 and 80 nm/ $\sqrt{s}$  at 973, 1073 and 1273 K, respectively. These data indicate that the expansion is attributed to the diffusion of radiation-induced defects, especially interstitials. The diameter of

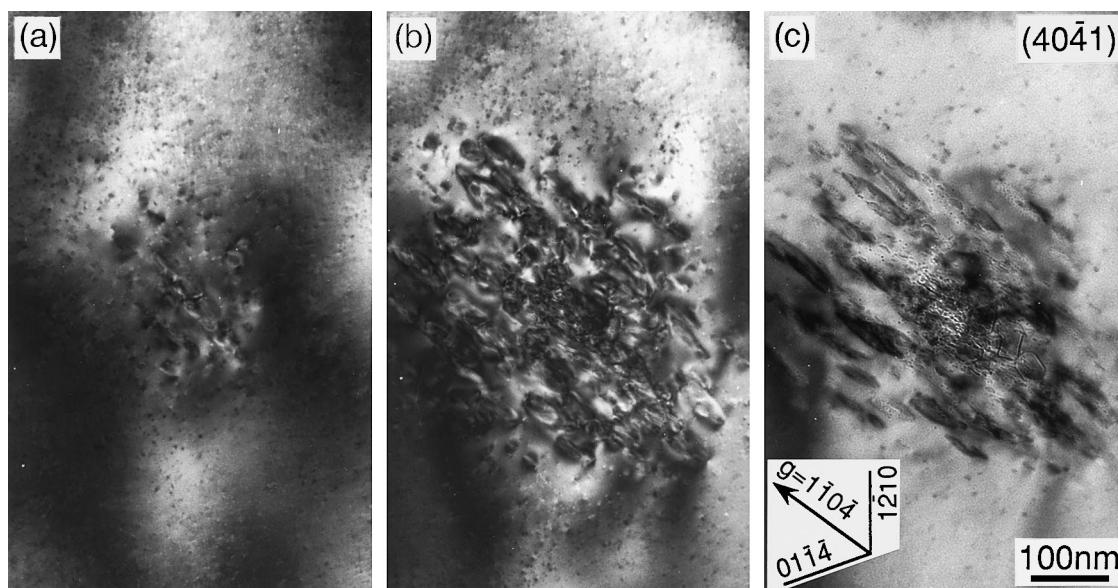


Fig. 1. Microstructures in the pure sample irradiated at 973 K to (a)  $1.2 \times 10^{26}$ , (b)  $6.0 \times 10^{26}$  and (c)  $7.2 \times 10^{26}$  e/m<sup>2</sup>.

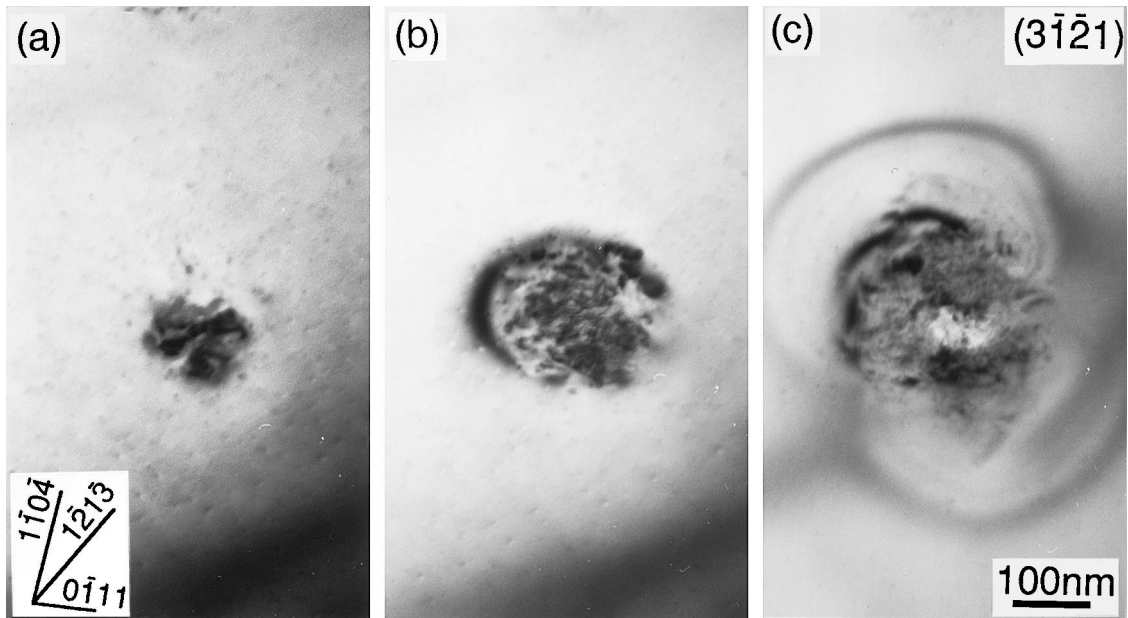


Fig. 2. Microstructures in the Cr<sub>2</sub>O<sub>3</sub>-doped sample irradiated at 973 K to (a)  $1.2 \times 10^{26}$ , (b)  $3.0 \times 10^{26}$  and (c)  $7.2 \times 10^{26}$  e/m<sup>2</sup>.

the damaged area in the Cr<sub>2</sub>O<sub>3</sub>-doped sample is also proportional to the square root of the irradiation time, but the proportional constants are about half of those in

the pure sample: 12, 19, 30 and 32.5 nm/ $\sqrt{s}$  at 973, 1073, 1173 and 1273 K, respectively.

The damaged area diameters at a dose of  $6 \times 10^{26}$  e/m<sup>2</sup> are demonstrated as a function of temperature in Fig. 4 for the pure, Cr<sub>2</sub>O<sub>3</sub>-doped and TiO<sub>2</sub>-doped samples. The damaged area expands rapidly above 973 K in the pure and TiO<sub>2</sub>-doped samples. However, the area is hardly changed by the irradiations from 293 to 973 K, and the increase of the diameter is small in the Cr<sub>2</sub>O<sub>3</sub>-doped sample. These results indicate that the mobility of radiation-produced interstitials was at 293 K in any of the three samples, but they migrated long distance at

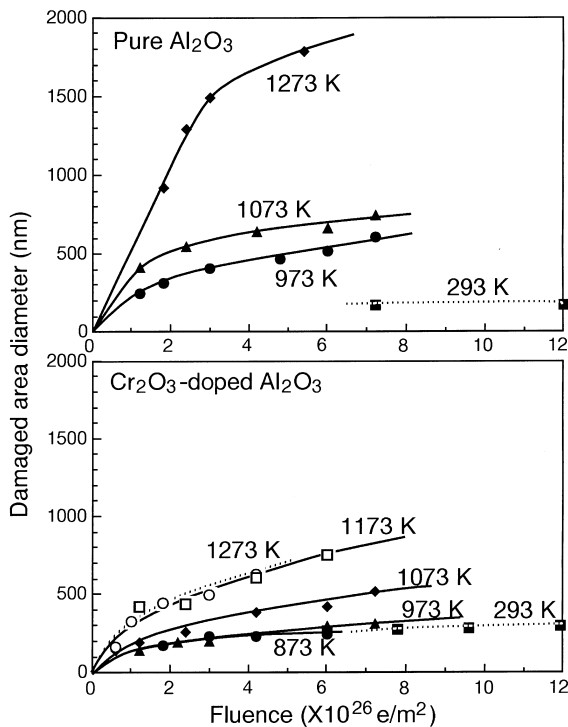


Fig. 3. Irradiation fluence dependence of the damaged area diameter at various temperatures in the pure and Cr<sub>2</sub>O<sub>3</sub>-doped samples.

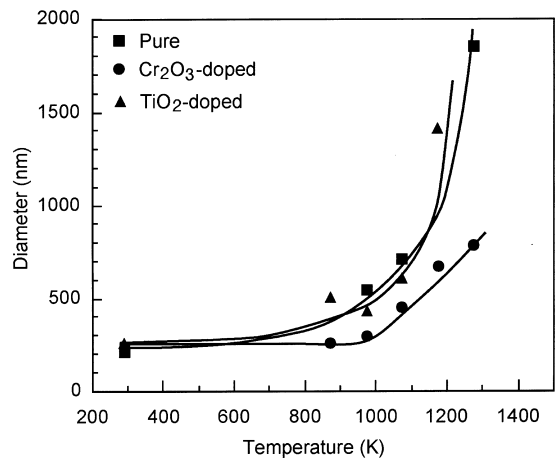


Fig. 4. Irradiation temperature dependence of the damaged area diameter in the pure, Cr<sub>2</sub>O<sub>3</sub>-doped and TiO<sub>2</sub>-doped samples irradiated to  $6 \times 10^{26}$  e/m<sup>2</sup>.

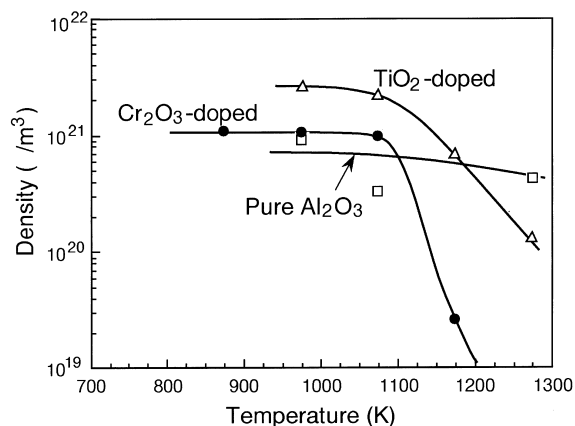


Fig. 5. Irradiation temperature dependence of the saturated loop density in the pure, Cr<sub>2</sub>O<sub>3</sub>-doped and TiO<sub>2</sub>-doped samples.

973 K and above in the pure and TiO<sub>2</sub>-doped samples. However, in the Cr<sub>2</sub>O<sub>3</sub>-doped sample, the mobility of interstitials is small below 973 K. Therefore, migration of radiation-induced defects seemed to be suppressed by the addition of Cr<sub>2</sub>O<sub>3</sub> to Al<sub>2</sub>O<sub>3</sub>.

The irradiation temperature dependence of dislocation loop density is shown in Fig. 5 for the pure, Cr<sub>2</sub>O<sub>3</sub>-doped and TiO<sub>2</sub>-doped samples. The loop density was measured in the central part of the damaged area. The density increases in the early stage of irradiation and reaches a constant value. The saturated loop densities are plotted in Fig. 5. The loop density in the TiO<sub>2</sub>-doped sample is three times higher than that in the pure sample at 973–1173 K, although these two samples have nearly the same expansion rates of damaged area during irradiation. Therefore, TiO<sub>2</sub> seems to act as a nucleation site for a dislocation loop. In the Cr<sub>2</sub>O<sub>3</sub>-doped sample, the

loop density of  $1 \times 10^{21}/\text{m}^3$  hardly changes at 873–1073 K, and it sharply drops to  $2 \times 10^{19}/\text{m}^3$  at 1173 K.

Cavity structures after irradiation to about  $7.2 \times 10^{26} \text{ e/m}^2$  at 1073 K are compared with the pure, Cr<sub>2</sub>O<sub>3</sub>-doped and TiO<sub>2</sub>-doped samples in Fig. 6. The cavities show an elliptical or irregular shape, lying on a basal plane in the pure sample. The size is distributed widely from about 5 to 40 nm, and the density and average diameter are  $1.2 \times 10^{22}/\text{m}^3$  and 11 nm at 1073 K, respectively. Some of the cavities are formed inside dislocation loops. As the micrograph of the TiO<sub>2</sub>-doped sample was observed parallel to a basal plane, the planar cavities formed on a basal plane are clearly observed. On the other hand, cavities are formed in a very high density in the Cr<sub>2</sub>O<sub>3</sub>-doped sample: the density is more than  $1 \times 10^{23}/\text{m}^3$  at 1073 K. However, the cavities retain a very small size of 3 nm after the  $7.2 \times 10^{26} \text{ e/m}^2$  irradiation, as they hardly grow with irradiation. So, the resultant volume swelling seems to be small compared with the pure and TiO<sub>2</sub>-doped samples. The irradiated areas are thinned during irradiation and finally are pitted in the Cr<sub>2</sub>O<sub>3</sub>-doped and TiO<sub>2</sub>-doped samples.

#### 4. Summary

In order to clarify the effects of Cr<sup>3+</sup> and Ti<sup>4+</sup> additions on damage structure development, pure and 1 mol%Cr<sub>2</sub>O<sub>3</sub>- or 1 mol%TiO<sub>2</sub>-doped Al<sub>2</sub>O<sub>3</sub> were irradiated with 400 keV electrons at temperatures from 293 to 1273 K.

In the pure sample, dislocation loops and plate-shaped cavities were formed on (0 0 0 1) planes. The damaged area, in which the loops were formed, expanded outward from the central part of the irradiation beam during irradiation above 973 K, while negligible expansion was seen in the 293 K irradiation. The

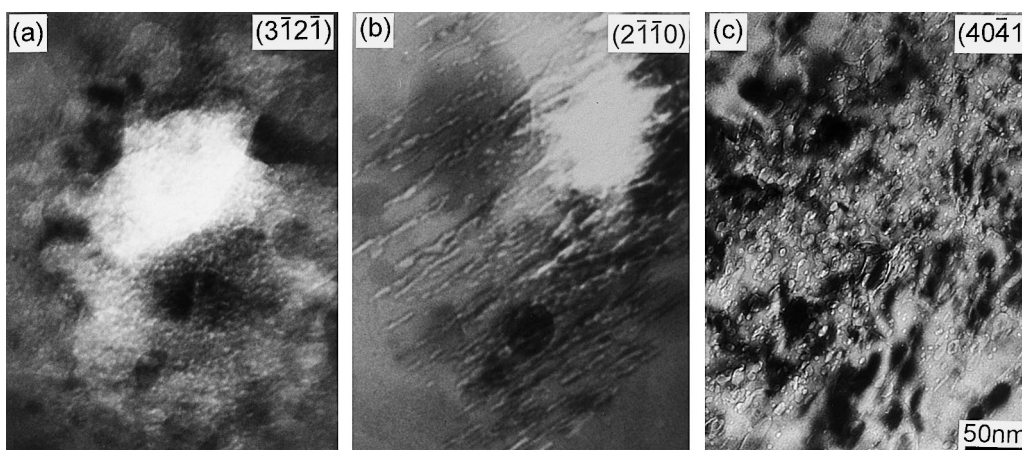


Fig. 6. Cavity structures in (a) the Cr<sub>2</sub>O<sub>3</sub>-doped, (b) TiO<sub>2</sub>-doped and (c) pure samples irradiated at 1073 K to  $7.2 \times 10^{26} \text{ e/m}^2$ .

expansion was attributed to the diffusion of radiation-produced defects, especially interstitials. Although the expansion of the damaged area was also observed in the Cr<sub>2</sub>O<sub>3</sub>-doped sample, the expansion occurred at temperatures higher than 1073 K and the expansion rate was smaller than that in the pure sample. The cavities were formed at a high density compared with pure sample, but they hardly grew with irradiation, which resulted in retention of a very small size at doses higher than  $7.2 \times 10^{26}$  e/m<sup>2</sup>. The dislocation loop and cavity formations in TiO<sub>2</sub>-doped sample were similar to those in the pure sample.

From these results, it was concluded that the migration of radiation-induced defects, especially interstitials, was suppressed by the addition of 1 mol% Cr<sub>2</sub>O<sub>3</sub>, resulted in retardation of the structural development due to irradiation. Therefore, the addition of Cr<sub>2</sub>O<sub>3</sub> would be expected to improve the radiation resistance of Al<sub>2</sub>O<sub>3</sub>. However, the TiO<sub>2</sub> addition showed little beneficial effect on the radiation damage of Al<sub>2</sub>O<sub>3</sub>.

#### Acknowledgements

The authors are grateful to Dr. H. Abe of JAERI for his invaluable help with the 400 kV TEM examinations.

#### References

- [1] W.J. Weber, L.K. Mansur, F.W. Clinard, Jr., D.M. Parkin, *J. Nucl. Mater.* 184 (1991) 1.
- [2] G.P. Pells, *J. Am. Ceram. Soc.* 77 (1994) 368.
- [3] F.W. Clinard, Jr., L.W. Hobbs, in: R.A. Johnson, A.N. Orlov (Eds.), *Physics of Radiation Effects in Crystals*, Elsevier, Amsterdam, 1986, p. 387.
- [4] Y. Katano, S.J. Zinkle, K. Nakata, A. Hishinuma, H. Ohno, *J. Nucl. Mater.* 212–215 (1994) 1039.
- [5] S.J. Zinkle, E.R. Hodgson, *J. Nucl. Mater.* 191–194 (1992) 58.
- [6] C. Kinoshita, *J. Nucl. Mater.* 191–194 (1992) 67.
- [7] G.P. Pells, M.J. Murphy, *J. Nucl. Mater.* 191–194 (1992) 621.
- [8] T. Shikama, G.P. Pells, *Philos. Mag. A* 47 (1983) 369.
- [9] M. Backhaus-Ricoult, S. Hagege, A. Peyrot, P. Moreau, *J. Am. Ceram. Soc.* 77 (1994) 423.
- [10] R.W. Klaffky, B.H. Rose, A.N. Goland, G.J. Dienes, *Phys. Rev. B* 21 (1980) 3610.
- [11] Y. Katano, K. Nakata, S. Kasahara, H. Ohno, *J. Nucl. Mater.* 191–194 (1992) 598.
- [12] Y. Katano, H. Ohno, H. Katsuta, *J. Nucl. Mater.* 155–157 (1988) 366.
- [13] W.E. Lee, K.P.D. Lagerlof, *J. Electron Microscopy Technol.* 2 (1985) 247.
- [14] G.P. Pells, D.C. Phillips, *J. Nucl. Mater.* 80 (1979) 215.